1   **Minimising the impact of biologging devices: Using Computational Fluid**

2   **Dynamics for optimising tag design and positioning**

3   William P. Kay[1,2,†,*], David S. Naumann[3,*], Hannah J. Bowen[3], Simon Withers[3], Benjamin

4   J. Evans[3], Rory P. Wilson[1], Thomas B. Stringell[4], James C. Bull[2], Phil W. Hopkins[1], Luca

5   Börger[1]

6   **Short/Running Title:** Minimising the impact of biologging devices

7

8   **Word count:** 7,999

9   [*]Both authors contributed equally.

10 [†]Corresponding author. E-mail: william.p.kay@swansea.ac.uk

11 [1]Swansea Laboratory for Animal Movement, Department of Biosciences, College of

12 Science, Swansea University, Swansea, SA2 8PP, Wales, UK

13 [2]Spatial & Population Ecology Research Group, Department of Biosciences, College of

14 Science, Swansea University, Swansea, SA2 8PP, Wales, UK

15 [3]Zienkiewicz Centre for Computational Engineering, College of Engineering, Swansea

16 University, SA1 8EN, UK

17 [4]Natural Resources Wales, Maes y Ffynnon, Penrhos Road, Bangor, Gwynedd, LL57

18 2DW, UK

19

20

Abstract

1. Biologging devices are used ubiquitously across vertebrate taxa in studies of movement and behavioural ecology to record data from organisms without the need for direct observation. Despite the dramatic increase in the sophistication of this technology, progress in reducing the impact of these devices to animals is less obvious, notwithstanding the implications for animal welfare. Existing guidelines focus on tag weight (e.g. the '5% rule'), ignoring aero/hydrodynamic forces in aerial and aquatic organisms, which can be considerable. Designing tags to minimise such impact for animals moving in fluid environments is not trivial, as the impact depends on the position of the tag on the animal, as well as its shape and dimensions.

2. We demonstrate the capabilities of computational fluid dynamics (CFD) modelling to optimize the design and positioning of biologgers on marine animals, using the grey seal (*Halichoerus grypus*) as a model species. Specifically, we investigate the effects of (i) tag form, (ii) tag size and (iii) tag position and quantify the impact under frontal hydrodynamic forces, as encountered by seals swimming at sea.

3. By comparing a conventional vs. a streamlined tag, we show that the former can induce up to 22% larger drag for a swimming seal; to match the drag of the streamlined tag, the conventional tag would have to be reduced in size by 50%. For the conventional tag, the drag induced can differ by up to 11% depending on the position along the seal's body, whereas for the streamlined tag this difference amounts to only 5%.

4. We conclude by showing how the CFD simulation approach can be used to optimise tag design to reduce drag for aerial and aquatic species, including issues such as the impact of lateral currents (unexplored until now). We also provide a step-by-step guide to facilitate implementation of CFD in biologging tag design.

47 **Second Language Abstract** (Welsh)

48 1. Defnyddir dyfeisiau biogofnodi'n eang iawn ar draws dosbarthiadau fertebratiaid

49 mewn astudiaethau symudiad ac ymddygiad ecolegol i gofnodi data o organeddau

50 heb fod angen arsylwi'n uniongyrchol. Er gwaethaf y cynnydd syfrdanol yn natur

51 soffistigedig y dechnoleg hon, mae'r cynnydd wrth leihau effaith y dyfeisiau hyn ar

52 anifeiliaid yn llai amlwg, er gwaethaf y goblygiadau ar gyfer lles anifeiliaid. Mae

53 canllawiau presennol yn canolbwyntio ar bwysau tag (e.e. y 'rheol 5%'), gan

54 anwybyddu grym aero/hydrodynamig mewn organeddau awyr a dyfrol, sy'n gallu bod

55 yn sylweddol. Nid yw dylunio tagiau i leihau effaith o'r fath i anifeiliaid sy'n symud

56 mewn amgylcheddau llifyddol yn beth bach, gan fod yr effaith yn dibynnu ar leoliad

57 y tag ar yr anifail, yn ogystal â'r siâp a'i ddimensiynau.

58 2. Rydym yn dangos galluoedd modelu deinameg hylif gyfrifiannol (CFD) i optimeiddio

59 dyluniad a lleoliad biogofnodwyr ar anifeiliaid morol, gan ddefnyddio'r morlo llwyd

60 (*Halichoerus grypus*) fel rhywogaeth fodel. Yn benodol, rydym yn ymchwilio i

61 effeithiau (i) ffurf y tag, (ii) maint y tag a (iii) lleoliad y tag a meintoli'r effaith dan

62 rymoedd hydrodynameg uniongyrchol, fel y mae morloi sy'n nofio yn y môr yn eu

63 profi.

64 3. Drwy gymharu tag confensiynol â thag llyfn, rydym yn dangos y gall y fersiwn

65 gonfensiynol greu hyd at 22% mwy o effaith lusgo i forlo sy'n nofio; er mwyn efelychu

66 effaith lusgo'r tag llyfn, byddai'n rhaid lleihau maint y tag confensiynol gan 50%. Ar

67 gyfer y tag confensiynol, gall yr effaith lusgo a grëir amrywio hyd at 11%, gan

68 ddibynnu ar ei leoliad ar gorff y morlo, er mai 5% yn unig yw'r gwahaniaeth hwn ar

69 gyfer tag llyfn.

70 4. Rydym yn cloi wrth ddangos sut gall ymagwedd efelychu CFD gael ei defnyddio i

71 optimeiddio dyluniad tagiau a lleihau'r effaith lusgo i rywogaethau awyr a dyfrol, gan

72 gynnwys materion megis effaith cerrynt ystlysol (nad ydynt wedi'u hastudio hyd yma).

73   Rydym hefyd yn cynnig canllaw cam wrth gam i hwyluso rhoi CFD ar waith wrth

74   ddylunio tagiau biogofnodi.

75   **Keywords:** animal welfare, biologging, biotelemetry, computational fluid dynamics, drag,

76   flow simulation, hydrodynamics, tag design

77

1   Introduction

79   In recent decades, the use of biologging devices to gather information on the behaviour,

80   movement and physiology of animals has increased substantially (Hussey et al. 2015).

81   In addition to collecting vast amounts of movement and behavioural data (Heylen &

82   Nachtsheim 2018), biologging devices can collect oceanographic data (Roquet et al.

83   2017; Treasure et al. 2017), and other environmental measures, such as ambient noise

84   levels (Mikkelsen et al. 2019). However, attachment of devices to animals is not without

85   consequence for the animals carrying them (Thorstad et al. 2001; Vandenabeele et al.

86   2014; Bodey et al. 2017; Wilson et al. 2018). Tag-induced detriment has often been

87   attributed to tag weight (Kenward 2001) which has driven researchers to work within

88   weight-defined bounds (Casper 2009). Indeed, researchers often select their study

89   animals based on the size or weight requirements for the tags, rather than trying to

90   optimise tags for a given species or size class; though there are examples of specific

91   developments made for very small animals (Stidsholt et al. 2018). Despite this, most

92   studies using tags have so far largely failed to take advantage of technological

93   advancements to reduce the impact of tags on animals (Portugal & White 2018).

94   Crucially, for projects involving tags on aerial and aquatic animals, the focus on weight

95   by most existing tag guidelines – e.g. the 3% or 5% rule (Casper 2009) – ignores

96   aero/hydrodynamic impacts (most notably drag) which are key in modulating energy

97   expenditure and behaviour during swimming (Culik & Wilson 1991; Cornick et al. 2006;

98 Rosen et al. 2017; van der Hoop et al. 2018), and flight (Bowlin et al. 2010; Pennycuick

99 et al. 2012; but see Tomotani et al. 2019). This may lead to biased data which is not

100 representative of freely moving animals (Ropert-Coudert et al. 2000; Barron et al. 2010;

101 Lear et al. 2018), as well as raising important ethical concerns for the animal being

102 tagged (Wilson & McMahon 2006).

103 Designing minimal-impact tags and testing drag in real systems is however not trivial, as

104 the impact is a complex function of both the position of the tag on the animal as well as

105 its shape and dimensions (Bannasch et al. 1994; Vandenabeele et al. 2015). One

106 approach to assess the effects of tag-induced drag is by *in-situ* modification of the shape

107 and positioning of tags deployed on a subject animal (or a model of it) in wind or flume

108 tunnels, or in captivity (Culik et al. 1994; van der Hoop et al. 2014; Shorter et al. 2017).

109 These approaches are beneficial insofar as during live experiments it is possible to

110 observe how animals react to tags under real operational conditions (cf. Pavlov &

111 Rashad 2012; van der Hoop et al. 2018), as well as assessing animal energetics, kinetics

112 and biomechanics, and changes in these over time (Geertsen et al. 2004; Ropert-

113 Coudert et al. 2007; Rosen et al. 2017; van der Hoop et al. 2018). However, experimental

114 approaches are limited in that they are very time consuming and labour intensive, wind

115 or flume tunnels are not always accessible, and the use of live animals raises ethical

116 concerns and requires appropriate licensing (Kyte et al. 2018). Furthermore, the logistical

117 constraints of working with very large taxa (e.g. cetaceans) often make *in-situ*

118 experiments impractical.

119 An alternative to experimental approaches uses computational fluid dynamics (CFD) to

120 assess tag-induced drag (Kyte et al. 2018). CFD is the primary tool for virtual design and

121 drag modelling within the aerospace industry (Jameson & Vassberg 2001) and is notable

122 in being able to model drag with the accuracy of results comparable to physical

123 experiments (Tyagi & Sen 2006; Jagadeesh et al. 2009; Vassberg et al. 2014); for

124 example Shorter et al. (2014) demonstrated that CFD simulation predictions of tag-

125 induced drag agreed with experimental assessments. Of particular value is that CFD

126 analysis can be implemented quickly and efficiently and can gather repeated,

127 comprehensive measures on aero/hydrodynamic aspects of tag design. As such, CFD

128 analysis can aid the prototyping of biologging tags prior to manufacture by estimating

129 their effects in a virtual environment without the need for experiments (Pavlov et al. 2007;

130 Kyte et al. 2018). Indeed, CFD has the potential to revolutionise biologging tag design

131 (Heylen & Nachtsheim 2018).

132 The use of CFD to examine tag design and impact has grown within the biologging

133 community since the mid-2000s (Pavlov et al. 2007) (see appendix S1 for a brief review).

134 Some commercial tag manufacturers utilise CFD to assess tags during product

135 development, though results from these studies are often not published. Indeed, the use

136 of CFD to examine tag-induced drag remains relatively limited in peer-reviewed

137 literature, and its full potential may not yet have been realised. Specifically, while there

138 have been several advances in the use of CFD to design tags and quantify their impact

139 (appendix S1), no publication has yet examined an approach which simultaneously

140 considers device size (Vandenabeele et al. 2015), shape (Shorter et al., 2014) and

141 positioning along the animal's body (Bannasch et al. 1994; Vandenabeele et al. 2014).

142 It is important to note that while the use of CFD to assess tag-induced drag is an

143 increasingly popular method, with clear advantages over experimental alternatives (Kyte

144 et al. 2018), it does have limitations, and one of our aims is to help ecologists become

145 aware of these and efficiently deal with them. Briefly, CFD analysis can be sensitive to

146 the choice of turbulence model; results may be specific to the particular tag and animal

147 geometries used in the study (thus care is required to compare results from different

148 studies); and geometric simplifications (such as the removal of antenna) are often

149 required during modelling, which will affect results. Further details of these limitations are

150 covered in appendix S2.

151 Nevertheless, provided potential limitations are acknowledged, CFD is an excellent tool

152 to test hypotheses at the level of concept (Pavlov & Rashad 2012), particularly if the aim

153 is, as is often the case (including in this study), to compare the drag of tagged versus

154 untagged animals, and to assess the effect of various designs, sizes and positions of

155 tags. CFD software is freely available for researchers, but its use has been largely

156 restricted to commercial tag manufacturers, individuals with substantial prior expertise,

157 or teams who are able to collaborate with aerospace engineers (Kyte et al. 2018).

158 Conversely, novice CFD users, like many ecologists, are not routinely able to implement

159 such techniques themselves.

160 Here we address this gap and support ecologists to realise the full potential of CFD for

161 improving tag design and assessing tag-induced drag. Specifically, we (i) evaluate how

162 tag-induced drag varies with device shape, size and positioning on the animal, (ii)

163 exemplify the efficacy of CFD for tag design, and (iii) provide step-by-step instructions

164 for ecologists to use CFD to efficiently assess the drag impact of biologging tags

165 (appendix S3); facilitating effective, future interdisciplinary collaborations with engineers.

166 **2   Materials and Methods**

167 In addition to this section, we provide a step-by-step guide to modelling the drag impact

168 of tags with CFD simulations using ANSYS FLUENT™, version R15.0 (ANSYS, Inc.,

169 Pennsylvania, USA) (appendix S3).

170 **2.1   Construction of geometries**

171 We used computer aided design (CAD) software (Autodesk® Inventor LT™, Autodesk

172 Inc., California, USA) to construct and manipulate seal and tag geometries. Note that

173　any modern 3D CAD software package will allow the geometric manipulations necessary

174　to reproduce this work. For the purpose of this study, two tag geometries were

175　considered. The first represented a traditional GPS tag for seals (tag A), as used in

176　Hazekamp et al. (2010), measuring 10 x 7 x 4 cm (length x width x height). The second

177　geometry represented a streamlined tag designed by us (tag B), measuring 11 x 10 x 4

178　cm. Both tags were designed to contain multiple biologging sensors capable of recording

179　data on seal movements and behaviour.

180　The seal geometry was obtained from Hazekamp et al. (2010) in IGES (.igs) format and

181　converted into a solid body for integration with the tag geometries. We chose to use the

182　seal and tag A geometries from Hazekamp et al. (2010) in order to facilitate direct

183　comparison of results. Importantly, the results from CFD simulations (see later) will

184　depend on (and be specific to) the chosen size of the animal geometry, hence the

185　geometry should be an appropriate reflection of the real animal being studied. Our seal

186　geometry was 1734 mm long – within the range of a typical adult female grey seal

187　(McLaren 1993). Our main aim was to exemplify the CFD method by assessing effects

188　of size, shape and position of the main body design of two tags on induced drag. Hence,

189　to maintain simplicity in the CFD modelling (cf. Kyte et al. 2018), external features such

190　as the antennae were removed from both tag geometries (see appendices S2 and S4

191　for details).

192　To prepare the geometries ahead of export to the CFD mesh generation process, we

193　used CAD 'cleaning' software (CADfix, International TechneGroup, Inc., Ohio, USA) to

194　ensure that the combined seal-tag solid body was 'watertight'. This is necessary to allow

195　the subsequent modelling of drag effects of the tag at different positions along the

196　animal's body.

197　**2.2　CFD simulations**

198   We undertook mesh generation, pre-processing and CFD simulations also within ANSYS

199   Fluent[TM]. We first undertook a mesh convergence study to determine the appropriate

200   mesh resolutions required for the simulations. We generated a surface mesh (Fig. 1),

201   encompassing the seal body and tag, composed of a finely resolved mesh for the fluid

202   boundary layer around the seal (Fig. 1 (a)), and a further (coarser) volume mesh for the

203   remainder of the volume around the seal body (Fig. 1(b)) (see appendix S4 for further

204   details). The surface mesh provided the input to ANSYS Fluent's numerical solver to

205   simulate the flow and determine flowfield properties, such as turbulence, around the

206   animal body under different freestream conditions, and to compute force coefficient

207   outputs. Importantly, the assumption was made that a steady-state solution existed for

208   each (non-dynamic) case, which allows for local time integration within the CFD solver,

209   as a precise time history of the solution was not necessary.

210   Flow visualisations were obtained using the software package *EnSight* and ANSYS

211   PostProcessing (ANSYS, Inc., Pennsylvania, USA), to provide a qualitative description

212   of the underlying fluid dynamics causing the force coefficient responses observed. A

213   summary of the CFD process is provided in Fig. 2 (and refer to appendix S4 for specific

214   details; see also appendix S3).

215   Simulations were undertaken using a range of flow speeds (1, 3, 5, 7 and 9 ms^{-1}) within

216   the typical range for simulation approaches for seals, including resultant speeds

217   encountered when seals swim into an oncoming flow, e.g. in high tidal flow environments

218   (Hazekamp et al. 2010; Kyte et al. 2018; Hastie et al. 2019). We computed non-

219   dimensional force coefficients in order to verify that non-dimensionalised outputs were

220   insensitive to the absolute input freestream velocity across this range; indeed, all force

221   coefficients collapsed onto a single curve across this speed range, indicating that the

222   force coefficient response was independent of freestream speed, and that our results

223   remained consistent across the range of velocities modelled. Thus, a velocity of 5 ms^{-1}

224   was selected for further investigation because we were particularly interested in the drag

225   effects and performance of tags when flow speed was relatively high; such speeds may

226   be encountered by seals swimming in highly tidal, fast flowing areas (Hastie et al. 2019).

227   In line with Pavlov & Rashad (2012) our model was assumed to represent an animal

228   swimming at a constant speed in a rectilinear fashion. While at sea, seals undertake a

229   range of complex 3D motions (Mitani et al. 2003) and move at varying speeds (Williams

230   2018). Hence, our results cannot account for the full range of movement that a seal

231   exhibits, but instead focus on the predominant forward motion of straight line swimming

232   that seals undertake during transit (Davis et al. 2001). These simplifications are

233   necessary due to the added complexity of modelling the highly unsteady and interacting

234   effects of fluid flow around a non-rigid, moving body (Adkins & Yan 2006); while these

235   analyses are possible and certainly interesting for future studies, they require the use of

236   unsteady, fluid-structure interaction CFD modelling techniques (Adkins & Yan 2006) and

237   were unnecessary for our aims (see also Kyte et al. 2018).

238   The output from the CFD simulations was the non-dimensional drag coefficient (C_d) for

239   each seal and tag combination. The Reynolds number, *Re*, of the flow simulations,

240   defined as

241     $$Re = \frac{\rho V L}{\mu} \qquad\qquad (1)$$

242   where ρ is the fluid density (1028 kg m^{-3}), V is the freestream flow velocity (5 m s^{-1}), L is

243   the seal length (1734 mm) and μ is the dynamic viscosity of salt water (1.09 x 10^{-3} Pa s),

244   was 8.2 x 10^6.

245   All non-dimensional drag coefficients, C_d, defined as

246     $$C_d = \frac{D}{\frac{1}{2}\rho V^2 A} \qquad\qquad (2)$$

247   where D is the absolute drag value (in Newtons) of each seal and tag combination, were

248   determined for each tag type, at nine discrete positions along the seal's dorsal surface,

249   under frontal flow (zero angle of attack) using the seal frontal area, A (0.134 m^2), as the

250   reference. The nine positions studied ranged from the seal's neck (position 1; 216 mm

251   from the nose) to 1080 mm from the nose (position 9) (Fig. 3). The comparisons of C_d

252   values are for the combined seal-tag body.

253   **2.3   The effect of tag size, shape and position on tag-induced drag**

254   To examine the effect of tag size, we used the non-dimensional drag coefficient (C_d),

255   hereon "drag", obtained from the CFD solver, to predict by how much the standard tag

256   (A) would need to be decreased in size in order to reduce its absolute drag penalty to

257   the same value of the more hydrodynamic tag B (under the same flow conditions). Thus,

258   via a process of linear re-scaling, we iteratively reduced the size of tag A to reach the

259   equivalent drag penalty to that of tag B.

260   We used a paired t-test to examine the effect of tag shape on tag-induced drag (i.e. mean

261   drag over the full range of nine positions modelled). To test the effect of tag positioning

262   *per se* we modelled drag as a function of position using a linear fixed-effects model (using

263   a cubic polynomial function to account for the non-linear effect of position), including tag

264   type (A or B) as a fixed effect (to account for shape effects), interacting with position. We

265   used step-wise model selection to compare the full model (with an interaction between

266   tag shape and position) vs the intercept only model, as well as comparing cubic vs

267   quadratic polynomial functions for the position covariate, retaining the former in both

268   cases. All analyses were performed using R version 3.5.1 (R Core Team 2018).

269   **3   Results**

270   We used CFD modelling to quantify the drag increase of tags on marine animals over

271   the baseline case of a non-tagged animal, using the grey seal as a model species. The

272   results presented in this section outline the effects of shape, size and positioning of two

273   contrasting tag types on the turbulence and pressures generated around the tag, and

274   hence the drag experienced by tagged animals.

275   **3.1   Turbulence and pressures generated by tags with contrasting shape**

276   Tag A, a standard tag, commonly used for seals and other marine mammals, with a non-

277   streamlined shape, induced considerably more turbulent distortions, particularly in the

278   wake of the device, than the streamlined tag B, with the reattachment point of the lowest,

279   smooth streamline passing over tag A 20% further downstream from the base of the tag

280   than in the case of tag B (Fig. 4). This delayed reattachment of streamlined flow results

281   in a turbulent wake region that is approximately 30% larger (when viewed transversely).

282   This type of drag is often referred to as 'base drag' (Suliman et al. 2009) and is one of

283   the major contributors to the increased drag of tag A. There are also stagnant, turbulent

284   flow regions on the upper side of tag A which are not evident on tag B (Fig. 4). These

285   stagnant regions (due to the less streamlined upper surface of tag A) contribute to

286   increased drag. The peak pressure on the front of tag A is 15% higher than that on tag

287   B and the high pressure region on tag A (see red area in Fig. 4) is 65% larger than that

288   on tag B. There is also evidence of a considerable low pressure (blue) region, generating

289   suction, on the upper surface of tag A which is not present on tag B. The general form of

290   the regions of high and low pressure across the tags was consistent across all positions

291   for both tag shapes (Fig. 4).

292   **3.2   Shape and size effects on drag experienced by tagged animals**

293   Tag A produced an 18.5% greater mean percentage drag increase than tag B across the

294   full range of positions studied (t = 16.012, df = 8, p < 0.001) (Table 1), with a maximum

295   percentage increase of 22.3% greater than tag B (at position 6) (Table 2). These results

296   mean that tag A would require a ca. 50% linear scaling reduction in size to reduce its

297   drag penalty to that of tag B; i.e. from 10 x 7 x 4 cm (c.f. Table 1) to 5 x 3.5 x 2 cm. It is

298   also worth noting that tag B is the preferred option for lower absolute drag despite it being

299   markedly larger than tag A.

300   ### 3.3   Position effects on drag experienced by tagged animals

301   The positioning of tags had a marked impact on their drag (Fig. 5) (Tag A: $F_3 = 25.253$,

302    $p < 0.001$; Tag B: $F_3 = 10.362$, $p < 0.001$). Positions 2 and 9 (on the dorsal surface at the

303   neck, and between the shoulder blades respectively; corresponding to 215.75 mm and

304   1083.44 mm from the tip (nose) of the model), were optimum for tag A and tag B,

305   respectively (Fig. 5). The drag varied non-linearly with positioning, and this effect differed

306   by tag type ($p = 0.002$). Drag was greatest around the mid-point of the dorsal surface on

307   the model seal (specifically, positions 5 and 6 for tag A, and positions 3 and 4 for tag B)

308   (Fig. 5; Table 2). Importantly, the variability in tag-induced drag between attachment

309   positions was markedly greater in tag A, with drag values ranging from 0.071 to 0.078;

310   equating to an increase in drag penalty, compared to a seal with no tag, of +20.8% to

311   +32.1%, with a maximum drag penalty difference of 11.3% between positions 2 and 6.

312   For tag B these values ranged from 0.063 to 0.066, equating to an increase in drag of

313   +6.5% to +11.9%, with a maximum difference of 5.4% between positions 4 and 9 (Table

314   2). Accordingly, the coefficient of variation in drag for tag A (3.31 %) was almost double

315   that of tag B (1.71 %).

316   ### 4   Discussion

317   We showed how CFD modelling can be used to quantify and reduce tag impact on

318   aquatic and aerial animals through virtual design testing. Using the example of tags

319   attached to grey seals, we showed how to evaluate and quantify the interacting effects

13

320   of tag shape, size and position on the magnitude of tag-induced drag. Our step-by-step

321   guide (appendix S3) provides a standardised framework for ecologists to use CFD to

322   assess the drag impact of tags, and more routinely report it in publications.

323   Tag A gave rise to a more turbulent flow disturbance, which also propagated over a

324   longer distance, than for tag B (Fig. 4). This contributed to the greater drag generated by

325   tag A (Table 1; 2). This increase in drag can also be attributed to the larger regions of

326   high (red) and low (blue) pressure differentials than for tag B (Fig. 4). This is in

327   accordance with other CFD and wind tunnel research on seals (Kyte et al., 2018),

328   cetaceans (Fiore et al. 2017) and birds (Vandenabeele et al. 2014), where greater

329   turbulent flow distortions and larger pressure differentials contributed to increased drag.

330   We note that the absolute drag values observed in our study are larger than those

331   obtained in Kyte et al. (2018), who modelled tag-induced drag on a similarly sized harp

332   seal. This can be attributed to the large difference in flow velocities used in the

333   simulations; Kyte et al. (2018) used a maximum flow velocity of 1.7 ms^{-1} whereas our

334   simulations used 5 ms^{-1}. Importantly, when scaled to non-dimensional drag, our values

335   are in line with that work. Likewise, when comparing our work to Hazekamp et al. (2010)

336   we found similar yet quantitatively different results. Specifically, Hazekamp et al. (2010)

337   observed a 13.8% increase in drag, whereas we saw an increase of 23.5%. This

338   difference is expected because Hazekamp et al. (2010) ran their simulations using the

339   *k-ε* turbulence model, which tends to underpredict the drag impact of a tag (see Kyte et

340   al. 2018 and appendix S2 for further details).

341   Tag A had a considerably larger low pressure region than tag B (Fig. 4) which could

342   negatively impact tagged animals by contributing to a lift force trying to pull the tag off

343   the animal (Fiore et al. 2017). High and low pressure differentials can act to increase

344   shear loading or downforce, which could cause injury at the site of attachment, or lead

345   to early detachment of a tag from an animal (Fiore et al. 2017). Hence, minimising drag

346 will likely also increase attachment time for suction cup tags (Pavlov et al. 2007; Fiore et

347 al. 2017). CFD modelling can also resolve lift forces and we note that both tags generated

348 substantial variation in lift coefficient (C_l) (Table 2), although the magnitude of C_l was

349 negligible compared to the drag. It was not a primary aim of ours to investigate C_l, hence

350 we reserve discussion of this to the supporting information (appendix S5).

351 Our comparison of two contrasting tag designs allowed us to exemplify that tag shape

352 may be more influential than size *per se* in generating increased drag for tagged animals,

353 with the considerably larger but more hydrodynamically designed tag (B) giving rise to a

354 lower drag penalty than the smaller tag A (Table 1). This result is in agreement with

355 Balmer et al. (2014) who demonstrated that the size of tags was an insignificant driver

356 of overall drag, with only a 1.2% increase in drag between the smallest (25 mm) and

357 largest (38.6 mm) tags studied. Thus, we propose that tag shape should be considered

358 more systematically (Fig 5-6) and we demonstrated how CFD simulations are ideal for

359 this. Moreover, achieving the reduction in size that would be necessary to reduce drag

360 without instead designing a more streamlined form (here a reduction in size of tag A by

361 ca. 50 %) is often not possible due to limitations in the size of electronic components and

362 batteries. On the contrary, our results suggest there may be scope to increase the size

363 of tags, within reason, providing that their form ultimately leads to a reduction in drag

364 (Fig. 6) – see also Shorter et al. (2014) and Fiore et al. (2017). Certainly, seen in this

365 light, the persistent stated aim to simply "miniaturise" biologging devices may be too

366 simplistic (Portugal & White 2018).

367 If tag size is to be increased, other factors such as minimizing the area of contact with

368 the animal (i.e. tag footprint) or the method of tag attachment must also be considered

369 (Shorter et al. 2014). This is because the direct attachment of tags to study animals has

370 been shown to disrupt thermoregulatory responses, or create superficial abrasions

371 (McCafferty et al. 2007; Field et al. 2012). For example, tags attached to juvenile grey

372 seals gave rise to a 23% greater heat-flux where devices were attached, compared to

373 areas of undisturbed fur, which was likely due to heat leakage around the attachment

374 site (McCafferty et al. 2007). Superficial abrasions were observed when tags were

375 attached to seals using a mesh attachment (Mazzaro & Dunn 2010), and the use of

376 epoxies to attach external devices to the pelage of animals has the potential to cause

377 burns at the site of attachment (Field et al. 2012). Larger tags, if attached by these

378 methods, would require larger meshes and greater quantities of epoxy. Hence,

379 minimising tag footprint is important, and this further exemplifies the usefulness of using

380 CFD to efficiently and quickly evaluate the pros and cons of different tag design and size

381 choices. It is also important to note that the effect of tag-induced drag is likely to be

382 greater as the ratio of tag to animal volume increases (Kyte et al. 2018), and minimising

383 tag frontal cross-sectional area should also be undertaken where possible (Rosen et al.

384 2017). Ultimately, to reduce drag, tags should be designed to be more streamlined in

385 line with the contours of the animal being tagged, to achieve smooth flow reattachment

386 downstream of the tag (see tag B; Fig. 4). For this, an increase in size (and thus volume

387 and/or cross-sectional area) could be justified.

388 We demonstrated that device positioning is crucial in determining tag-induced drag, as

389 evidenced by the non-linear relationship between drag and tag position (Fig. 5). This

390 concurs with the results of Vandenabeele et al. (2014) who observed strong and non-

391 linear effects of tag position on induced drag on a model cormorant in a wind tunnel.

392 Similarly, Tudorache et al. (2014) documented that for swimming eels tagged with

393 biologging devices, placement of a tag in a non-optimum position, compared to an

394 optimum position, could result in a 15% reduction in critical swimming speed and a

395 significant increase in oxygen consumption rate while swimming. Our results also

396 showed that the effect of tag positioning on drag is significantly dependent upon the

397 shape of the tag, and that the variability in the effect of tag positioning for tag B is almost

398   half that for tag A. This demonstrates that improving hydrodynamic design can reduce

399   the impact of positioning *per se* on device-induced drag.

400   In practice, the choice of tag positioning will also depend on the form of the animal and

401   is further compounded by the fact that the positioning of a tag can affect both the quality

402   and quantity of data collected (Watson & Granger 1998; Jones et al. 2011). For example,

403   GPS data from marine animals can only be obtained when individuals surface for a long

404   enough duration to receive a satellite fix, and for this reason tags are routinely placed on

405   areas of the animal that are exposed most frequently and for the longest periods, for

406   example on the head of pinnipeds (Lake et al. 2006). This is pertinent also for

407   researchers deploying satellite transmitting devices with the aim of maximising the

408   number of successful transmissions, such as uplinks to the Argos network (Service

409   Argos, Toulouse, France). In such cases it may be that the optimum position of the tag

410   for data acquisition or transmission purposes could well be the least suitable position for

411   minimising drag (Watson & Granger 1998; Jones et al. 2011). In such cases, researchers

412   must consider the trade-offs of successful data acquisition with device effects, or

413   consider how they might modify their tags to achieve a more desirable outcome (Jones

414   et al. 2011); for example, researchers could consider using alternative technologies,

415   such as Fastloc-GPS devices, that require only very short durations at the surface (< 1

416   s) to acquire satellite fixes (Dujon et al. 2014), so that tags can be placed at optimum

417   (i.e. drag-minimising) positions on the animal that are exposed for shorter durations. The

418   method of attachment will also determine how accurately the tag can be positioned and

419   orientated on the animal. For example, tags that are attached by hand (such as tags

420   glued to seals) can be positioned more accurately than a tag attached using a pole e.g.

421   to a cetacean, (Stimpert et al. 2013). The position of tags may also shift during their

422   attachment period (e.g. suction cup tags). CFD offers the opportunity to explore the effect

423 of drag of tags positioned anywhere and in any orientation on the subject animal (Fiore

424 et al. 2017).

425 Tag position also affects the signals that are recorded - consider for example an

426 accelerometer: the signal received from a device placed on the head will be very different

427 to that of the same device placed on the back of an animal, given that accelerometers

428 are sensitive to tag orientation (Shepard et al. 2008). This factor would likely also play a

429 part in determining the final choice of device positioning. Managing these trade-offs is

430 challenging and requires that ecologists understand the behaviour of their study species

431 and the functioning of their tag, so that they can make appropriate decisions about where

432 to position a device and understand the drag-impacts of their choices (Jones et al. 2011);

433 this can be fully explored for different species and different devices using CFD.

434 Projects involving tag deployments are diverse and it is not always possible for

435 researchers to rely solely on "off-the-shelf" tags purchased from commercial companies,

436 with many researchers instead resorting to building their own (Kwok 2017). However,

437 there is currently limited advice for researchers who are developing their own tags about

438 how to quantify the drag of their tags and hence how to minimise impact. Here, we fill

439 this gap by providing a step-by-step guide that ecologists can follow to assess tag-

440 induced drag in a quick and efficient manner using CFD techniques (appendix S3), which

441 will aid more researchers to report on the drag-impact of their tags. The guide is written

442 for use with the standard CFD software ANSYS Fluent, used also by other ecologists

443 (Pavlov et al. 2007; Hazekamp et al. 2010), and guides users through the process of

444 modelling the drag impact of tags, from importing the tag design and animal geometry

445 files into the software, through setting up the computational environment and on to

446 running the CFD simulations. The guide will also help in establishing interdisciplinary

447 collaborations with engineers, and aid researchers across the biologging community to

448 increase their understanding of tag-induced drag and work towards best practices in tag

449   design, without the need to rely on collecting logistically challenging empirical data, for

450   example through the use of wind tunnel experiments (Vandenabeele et al. 2014).

451   In this study, we have focused on measuring drag with respect to frontal flow, i.e. a rigid

452   (or stationary) seal in a field of non-turbulent water (steady-state assumption), including

453   at different flow velocities. This modelling approach can be extended to consider lateral

454   flow, as seals also perform turns or may swim at an angle relative to water current (and

455   in doing so can experience lateral hydrodynamic drag forces). Note that this is different

456   to changing the orientation of the tag on the animal, as demonstrated by Shorter et al.

457   (2014). The drag forces incurred by tags are likely to change markedly in each of these

458   circumstances and hence are also important to bear in mind. Such investigations can be

459   undertaken with a simple extension of our step-by-step guide, by rotating the model

460   animal in the computational environment so that it is lateral to the oncoming flow (see

461   appendix S6 for a first investigation of this).

462   The CFD method presented here offers a quick and efficient way to determine the best

463   tag (for reducing drag) for the animal being studied, by considering multiple factors

464   including tag design, size and position. However, researchers planning on using CFD

465   must be aware of its limitations. CFD relies on approximate, numerical solutions to the

466   governing fluid dynamic equations, and so there will always be some discrepancies in

467   absolute force predictions between independent studies; we have highlighted some key

468   comparisons between our results and those of similar works (Hazekamp et al. 2010; Kyte

469   et al. 2018). We provide necessary further detail on the limitations of CFD in appendix

470   S2, which we encourage the reader to consult for guidance.

471   This work has demonstrated the value of an interdisciplinary approach, harnessing

472   engineering techniques to design minimal impact tags and efficiently assess their relative

473   drag loading. While CFD has previously been utilised to measure the impact of tags

474   (appendix S1), its use has largely been limited to researchers with substantial prior CFD

475   modelling expertise (Kyte et al. 2018). The methods we use here are standard for

476   aeronautical design (Jameson & Vassberg 2001) and our guide offers new opportunities

477   for further collaboration between engineers and ecologists - particularly for researchers

478   novice to CFD techniques.

479   Finally, most existing guidelines for tag impact do not advise on appropriate tag size,

480   placement positions or configurations (Rosen et al. 2017) and many are relatively naïve

481   to the impacts of drag that are most relevant to marine and aerial applications (see

482   appendix S7 for an overview). We anticipate that the reporting of drag values in future

483   publications may help improve future guidelines and address recent requests in the

484   literature for improved reporting of impacts (Bodey et al. 2017; Lameris & Kleyheeg 2017)

485   and better assessment of tag-induced effects (such as drag) prior to deployment in the

486   field (Lear et al., 2018). Whilst we do not expect our findings to be taken up as formal

487   guidelines, nor the use of CFD to be made compulsory, we hope that this work, and

488   specifically our step-by-step guide (appendix S3), will aid the biologging community in

489   achieving this.

490   **Acknowledgements**

496   **Author Contributions**

497 WPK, DSN, BJE, RPW, LB, TBS, JCB conceived and designed the research; DSN, BJE,

498 HB, SW and WPK undertook the analyses, with feedback from WPK, LB and RPW. WPK

499 led the writing of the manuscript. DSN, BJE, HB and SW wrote the step-by-step guide to

500 running the CFD simulations. PH created the tag B geometry. LB, RPW, DSN, BJE, JCB

501 and TBS contributed critically to manuscript drafts. All authors gave final approval for

502 publication.

Data Accessibility

504 Data are available from figshare: https://doi.org/10.6084/m9.figshare.8152943. These

505 data are under embargo until 1 August 2019.

References

507 Adkins, D., & Yan, Y. Y. (2006). CFD simulation of fish-like body moving in

508 viscous liquid. *Journal of Bionic Engineering*, *3*(3), 147–153.

509 Balmer, B. C., Wells, R. S., Howle, L. E., Barleycorn, A. A., McLellan, W. A.,

510 Ann Pabst, D., … Zolman, E. S. (2014). Advances in cetacean telemetry: A

511 review of single-pin transmitter attachment techniques on small cetaceans

512 and development of a new satellite-linked transmitter design. *Marine

513 Mammal Science*, *30*(2), 656–673.

514 Bannasch, R., Wilson, R. P., & Culik, B. (1994). Hydrodynamic aspects of

515 design and attachment of a back-mounted device in penguins. *The Journal

516 of Experimental Biology*, *194*(1), 83–96.

517 Barron, D. G., Brawn, J. D., & Weatherhead, P. (2010). Meta-analysis of

518 transmitter effects on avian behaviour and ecology. *Methods in Ecology*

519   *and Evolution*, *1*(2), 180–187.

520   Bodey, T. W., Cleasby, I. R., Bell, F., Parr, N., Schultz, A., Votier, S. C., &

521   Bearhop, S. (2017). A Phylogenetically Controlled Meta-Analysis of

522   Biologging Device Effects on Birds: Deleterious effects and a call for more

523   standardized reporting of study data. *Methods in Ecology and Evolution*,

524   *12*(10), 3218–3221.

525   Bowlin, M. S., Henningsson, P., Muijres, F. T., Vleugels, R. H. E., Liechti, F., &

526   Hedenström, A. (2010). The effects of geolocator drag and weight on the

527   flight ranges of small migrants. *Methods in Ecology and Evolution*, *1*(4),

528   398–402.

529   Casper, R. M. (2009). Guidelines for the instrumentation of wild birds and

530   mammals. *Animal Behaviour*, *78*(6), 1477–1483.

531   Cornick, L. A., Inglis, S. D., Willis, K., & Horning, M. (2006). Effects of increased

532   swimming costs on foraging behavior and efficiency of captive Steller sea

533   lions: Evidence for behavioral plasticity in the recovery phase of dives.

534   *Journal of Experimental Marine Biology and Ecology*, *333*(2), 306–314.

535   Culik, B. M., Bannasch, R., & Wilson, R. P. (1994). External devices on

536   penguins: How important is shape? *Marine Biology*, *118*, 353–357.

537   Culik, B., & Wilson, R. P. (1991). Swimming energetics and performance of

538   instrumented adelie penguins (*Pygoscelis adeliae*). *Journal of Experimental*

539   *Biology*, *158*, 355–368.

540   Davis, R. W., Fuiman, L. A., Williams, T. M., & Le Boeuf, B. J. (2001). Three-

541 dimensional movements and swimming activity of a northern elephant seal.

542 *Comparative Biochemistry and Physiology - A Molecular and Integrative*

543 *Physiology*, *129*(4), 759–770.

544 Dujon, A. M., Lindstrom, R. T., & Hays, G. C. (2014). The accuracy of Fastloc-

545 GPS locations and implications for animal tracking. *Methods in Ecology*

546 *and Evolution*, *5*(11), 1162–1169.

547 Field, I. C., Harcourt, R. G., Boehme, L., De Bruyn, P. J. N., Charrassin, J. B.,

548 Mcmahon, C. R., … Hindell, M. A. (2012). Refining instrument attachment

549 on phocid seals. *Marine Mammal Science*, *28*(3), 325–332.

550 Fiore, G., Anderson, E., Garborg, C. S., Murray, M., Johnson, M., Moore, M. J.,

551 … Shorter, K. A. (2017). From the track to the ocean: Using flow control to

552 improve marine bio-logging tags for cetaceans. *PLoS ONE*, *12*(2), 1–19.

553 Geertsen, B. M., Teilmann, J., Kastelein, R. A, Vlemmix, H. N. J., & Miller, L. A.

554 (2004). Behaviour and physiological effects of transmitter attachments on a

555 captive harbour porpoise (Phocoena phocoena). *Journal of Cetacean*

556 *Research and Management*, *6*(2), 139–146.

557 Hastie, G. D., Bivins, M., Coram, A., Gordon, J., Jepp, P., MacAulay, J., …

558 Gillespie, D. (2019). Three-dimensional movements of harbour seals in a

559 tidally energetic channel: Application of a novel sonar tracking system.

560 *Aquatic Conservation: Marine and Freshwater Ecosystems*,

561 doi:10.1002/aqc.3017

562 Hazekamp, A. A. H., Mayer, R., & Osinga, N. (2010). Flow simulation along a

563   seal: The impact of an external device. *European Journal of Wildlife*

564   *Research*, *56*(2), 131–140.

565   Heylen, B. C., & Nachtsheim, D. A. (2018). Bio-telemetry as an essential tool in

566   movement ecology and marine conservation. In YOUMARES 8–Oceans

567   Across Boundaries: Learning from each other (pp. 83-107). Springer,

568   Cham.

569   Hussey, N. E., Kessel, S. T., Aarestrup, K., Cooke, S. J., Cowley, P. D., Fisk, A.

570   T., … Whoriskey, F. G. (2015). Aquatic animal telemetry: A panoramic

571   window into the underwater world. *Science*, *348*(6240), 1255642.

572   Jagadeesh, P., Murali, K., & Idichandy, V. G. (2009). Experimental investigation

573   of hydrodynamic force coefficients over AUV hull form. *Ocean Engineering*,

574   *36*, 113–118.

575   Jameson, A., & Vassberg, J. (2001). Computational fluid dynamics for

576   aerodynamic design: Its current and future impact. In *39th Aerospace*

577   *Sciences Meeting and Exhibit*, p. 538.

578   Jones, T., Bostrom, B., Carey, M., Imlach, B., Mikkelsen, J., Ostafichuk, P., …

579   Jones, D. (2011). Determining Transmitter Drag and Best-Practice

580   Attachment Procedures for Sea Turtle Biotelemetry. *NOAA Technical*

581   *Memorandum*, *NMFS-SWFSC*.

582   Kenward, R. (2001). *A manual for wildlife radio tagging*. Academic Press.

583   Kwok, R. (2017). Field Instruments: Build it yourself. *Nature*, *545*(7653), 253–

584   255.

585   Kyte, A., Pass, C., Pemberton, R., Sharman, M., & McKnight, J. C. (2018). A

586   computational fluid dynamics (CFD) based method for assessing the

587   hydrodynamic impact of animal borne data loggers on host marine

588   mammals. *Marine Mammal Science*, doi:10.1111/mms.12540

589   Lake, S., Burton, H., & Wotherspoon, S. (2006). Movements of adult female

590   Weddell seals during the winter months. *Polar Biology*, *29*(4), 270–279.

591   Lameris, T. K., & Kleyheeg, E. (2017). Reduction in adverse effects of tracking

592   devices on waterfowl requires better measuring and reporting. *Animal*

593   *Biotelemetry*, *5*(1), 24.

594   Lear, K. O., Gleiss, A. C., & Whitney, N. M. (2018). Metabolic rates and the

595   energetic cost of external tag attachment in juvenile blacktip sharks

596   *Carcharhinus limbatus. Journal of Fish Biology*, *93*(2), 391–395.

597   Mazzaro, L. M., & Dunn, J. L. (2010). Descriptive account of long-term health

598   and behavior of two satellite-tagged captive harbor seals *Phoca vitulina*.

599   *Endangered Species Research*, *10*(1), 159–163.

600   McCafferty, D. J., Currie, J., & Sparling, C. E. (2007). The effect of instrument

601   attachment on the surface temperature of juvenile grey seals (*Halichoerus*

602   *grypus*) as measured by infrared thermography. *Deep-Sea Research Part*

603   *II: Topical Studies in Oceanography*, *54*(3–4), 424–436.

604   McLaren, I. A. (1993). Growth in pinnipeds. *Biological Reviews*, *68*(1), 1–79.

605   Mikkelsen, L., Johnson, M., Wisniewska, D. M., van Neer, A., Siebert, U.,

606   Madsen, P. T., & Teilmann, J. (2019). Long-term sound and movement

25

607   recording tags to study natural behavior and reaction to ship noise of seals.

608   *Ecology and Evolution, 9*(5), 2588-2601.

609   Mitani, Y., Sato, K., Ito, S., Cameron, M. F., Siniff, D. B., & Naito, Y. (2003). A

610   method for reconstructing three-dimensional dive profiles of marine

611   mammals using geomagnetic intensity data: results from two lactating

612   Weddell seals. *Polar Biology, 26*(5), 311–317.

613   Pavlov, V. V., Wilson, R. P., & Lucke, K. (2007). A new approach to tag design

614   in dolphin telemetry: Computer simulations to minimise deleterious effects.

615   *Deep-Sea Research Part II: Topical Studies in Oceanography, 54*(3–4),

616   404–414.

617   Pavlov, V. V., & Rashad, A. M. (2012). A non-invasive dolphin telemetry tag:

618   Computer design and numerical flow simulation. *Marine Mammal Science,*

619   *28*(1), 16–27.

620   Pennycuick, C. J., Fast, P. L. F., Ballerstädt, N., & Rattenborg, N. (2012). The

621   effect of an external transmitter on the drag coefficient of a bird's body, and

622   hence on migration range, and energy reserves after migration. *Journal of*

623   *Ornithology, 153*(3), 633–644.

624   Portugal, S. J., & White, C. R. (2018). Miniaturisation of biologgers is not

625   alleviating the 5% rule. *Methods in Ecology and Evolution, 1*(1), 1–2.

626   R Core Team. (2018). *R: A Language and Environment for Statistical*

627   *Computing.* R Foundation for Statistical Computing, Vienna. URL

628   http://www.R-project.org

629   Ropert-Coudert, Y., Knott, N., Chiaradia, A., & Kato, A. (2007). How do different

630   data logger sizes and attachment positions affect the diving behaviour of

631   little penguins? *Deep-Sea Research Part II: Topical Studies in*

632   *Oceanography*, *54*(3–4), 415–423.

633   Ropert-Coudert, Y., Bost, C., Handrich, Y., Bevan, R. M., Butler, P. J., Woakes,

634   A. J., & Le Maho, Y. (2000). Impact of Externally Attached Loggers on the

635   Diving Behaviour of the King Penguin. *Physiological and Biochemical*

636   *Zoology*, *73*(4), 438–444.

637   Roquet, F., Boehme, L., Block, B., Charrassin, J.-B., Costa, D., Guinet, C., …

638   Fedak, M. A. (2017). Ocean Observations Using Tagged Animals.

639   *Oceanography*, *30*(2), 139–139.

640   Rosen, D. A. S., Gerlinsky, C. G., & Trites, A. W. (2017). Telemetry tags

641   increase the costs of swimming in northern fur seals, *Callorhinus ursinus*.

642   *Marine Mammal Science*, 1–18.

643   Shepard, E., Wilson, R., Quintana, F., Gómez Laich, A., Liebsch, N., Albareda,

644   D., … McDonald, D. (2008). Identification of animal movement patterns

645   using tri-axial accelerometry. *Endangered Species Research*, *10*, 47–60.

646   Shorter, A., Murray, M., Johnson, M., Moore, M., & Howle, L. (2014). Drag of

647   suction cup tags on swimming animals: Modeling and measurement.

648   *Marine Mammal Science*, *30*(2), 726–746.

649   Shorter, A., Shao, Y., Ojeda, L., Barton, K., Rocho-Levine, J., van der Hoop, J.,

650   & Moore, M. (2017). A day in the life of a dolphin: Using bio-logging tags for
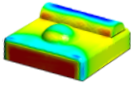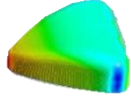
651   improved animal health and well-being. *Marine Mammal Science*, *33*(3),

652   785–802.

653   Stidsholt, L., Johnson, M., Beedholm, K., Jakobsen, L., Kugler, K., Brinkløv, S.,

654   … Madsen, P. T. (2018). A 2.6-g sound and movement tag for studying the

655   acoustic scene and kinematics of echolocating bats. *Methods in Ecology*

656   *and Evolution*, *10*(1), 48-58.

657   Stimpert, A. K., Mattila, D., Nosal, E. M., & Au, W. W. L. (2013). Tagging young

658   humpback whale calves: Methodology and diving behavior. *Endangered*

659   *Species Research*, *19*(1), 11–17.

660   Suliman, M. A., Mahmoud, O. K., Al-Sanabawy, M. A., & Abdel-Hamid, O. E.

661   (2009). Computational investigation of base drag reduction for a projectile

662   at different flight regimes. *Paper: ASAT-13-FM-05, 13th International*

663   *Conference on Aerospace Science and Aviation Technology, Military*

664   *Technical College, Kobry Elkobbah, Cairo, Egypt.*

665   Thorstad, E. B., Okland, F., & Heggberget, T. G. (2001). Are long term negative

666   effects from external tags underestimated? Fouling of an externally

667   attached telemetry transmitter. *Journal of Fish Biology*, *59*(4), 1092–1094.

668   Tomotani, B. M., Bil, W., Jeugd, H. P., Pieters, R. P. M., & Muijres, F. T. (2019).

669   Carrying a logger reduces escape flight speed in a passerine bird, but

670   relative logger mass may be a misleading measure of this flight

671   performance detriment. *Methods in Ecology and Evolution*, *10*(1), 70–79.

672   Treasure, A., Roquet, F., Ansorge, I. J., Bester, M., Boehme, L., Bornemann,

673   H., … de Bruyn, P. J. N. (2017). Marine mammals exploring the oceans

674   pole to pole: A review of the MEOP Consortium. *Oceanography*, *30*(2),

675   132–138.

676   Tudorache, C., Burgerhout, E., Brittijn, S., & Van Den Thillart, G. (2014). The

677   effect of drag and attachment site of external tags on swimming eels:

678   Experimental quantification and evaluation tool. *PLoS ONE*, *9*(11), 1–10.

679   Tyagi, A., & Sen, D. (2006). Calculation of transverse hydrodynamic coefficients

680   using computational fluid dynamic approach. *Ocean Engineering*, *33*, 798–

681   809.

682   van der Hoop, J. M., Fahlman, A., Hurst, T., Rocho-Levine, J., Shorter, K. A.,

683   Petrov, V., & Moore, M. J. (2014). Bottlenose dolphins modify behavior to

684   reduce metabolic effect of tag attachment. *Journal of Experimental Biology*,

685   *217*(23), 4229–4236.

686   van der Hoop, J. M., Fahlman, A., Shorter, K. A., Gabaldon, J., Rocho-Levine,

687   J., Petrov, V., & Moore, M. J. (2018). Swimming Energy Economy in

688   Bottlenose Dolphins Under Variable Drag Loading. *Frontiers in Marine*

689   *Science*, doi:10.3389/fmars.2018.00465

690   Vandenabeele, S., Grundy, E., Friswell, M., Grogan, A., Votier, S., & Wilson, R.

691   (2014). Excess baggage for birds: Inappropriate placement of tags on

692   gannets changes flight patterns. *PLoS ONE*, *9*(3).

693   Vandenabeele, S. P., Shepard, E. L. C., Grémillet, D., Butler, P. J., Martin, G.

694   R., & Wilson, R. P. (2015). Are bio-telemetric devices a drag? Effects of

695   external tags on the diving behaviour of great cormorants. *Marine Ecology*

696   *Progress Series*, *519*, 239–249.

697   Vassberg, J. C., Tinoco, E. N., Mani, M., Rider, B., Zickuhr, T., Levy, D. W., …

698   Murayama, M. (2014). Summary of the Fourth AIAA Computational Fluid

699   Dynamics Drag Prediction Workshop. *Journal of Aircraft*, *51*(4), 1070–

700   1089.

701   Watson, K. P., & Granger, R. A. (1998). Hydrodynamic effect of a satellite

702   transmitter on a juvenile green turtle (*Chelonia mydas*). *Journal of*

703   *Experimental Biology*, *201*(17), 2497–2505.

704   Williams, T.M. (2018). Swimming. In E*ncyclopedia of marine mammals* (pp.

705   970-979). Academic Press.

706   Wilson, R. P., Holton, M., Wilson, V. L., Gunner, R., Tysse, B., Wilson, G. I., …

707   Scantlebury, D. M. (2018). Towards informed metrics for examining the role

708   of human-induced animal responses in tag studies on wild animals.

709   *Integrative Zoology*, *14*(1), 17-29.

710   Wilson, Rory P., & McMahon, C. R. (2006). Measuring devices on wild animals:

711   What constitutes acceptable practice? *Frontiers in Ecology and the*

712   *Environment*, *4*(3), 147–154.

713

714 **Tables**

715 Table 1. The dimensions, volume, drag coefficient (C_d) (mean ± standard deviation) and

716 percentage increase in C_d over the baseline case (seal with no tag) (mean ± standard

717 deviation) of tag designs A and B. Means and percentage increase of drag are calculated
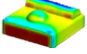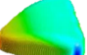
718 over the range of positions tested (1-9).

Tag	Form	Dimensions (L x W x H; cm)	Volume (cm^3)	Drag coefficient (C_d) (mean ± SD)	Drag coefficient % increase over the baseline (no tag) case (mean ± SD)
A		10 x 7 x 4	280	0.075 ± 0.002	27.4 ± 4.2
B		11 x 10 x 4	440	0.064 ± 0.001	8.9 ± 1.8

719

720 Table 2. The drag force (N), power requirement (W), drag coefficient (C_d), and percentage increase of C
721 baseline case (seal with no tag), across all positions. Note that negative C_l values equates to downfor
722 Results shown are for the simulations at 5 ms^{-1} but apply equally across all swim speeds tested (see Met

Tag	Position	Position (mm)	Drag (N)	Power (W)	Drag coefficient (C_d)	C_d increase over baseline case (seal with no tag) (%)	L coef (
None	NA	NA	101.3	506.6	0.0588	NA	0.0
A	1	215.75	125.1	625.5	0.0726	23.5	0.0
A	2	325.37	122.5	612.3	0.0711	20.9	0.0
A	3	411.47	127.0	635.0	0.0737	25.3	0.0
A	4	580.60	132.5	662.6	0.0769	30.8	0.0
A	5	667.69	133.8	669.1	0.0777	32.1	0.0
A	6	783.83	133.9	669.5	0.0777	32.1	0.0
A	7	900.90	131.7	658.3	0.0764	29.9	0.0
A	8	968.21	130.6	653.1	0.0758	28.9	-0.0
A	9	1083.44	125.1	625.5	0.0726	23.5	-0.0
B	1	215.75	108.4	542.1	0.0629	7.0	-0.0
B	2	325.37	109.8	548.8	0.0637	8.3	0.00
B	3	411.47	112.0	560.0	0.0650	10.5	0.00
B	4	580.60	113.4	566.9	0.0658	11.9	0.00
B	5	667.69	112.0	560.0	0.065	10.5	-0.0
B	6	783.83	111.3	556.6	0.0646	9.9	-0.0
B	7	900.90	109.8	548.8	0.0637	8.3	0.00
B	8	968.21	108.9	544.5	0.0632	7.5	0.00
B	9	1083.44	107.9	539.4	0.0626	6.5	0.00

723